Journal of Alzheimer's Disease xx (20xx) x–xx
DOI 10.3233/JAD-122431
IOS Press

The Pattern of Diffusion Parameter Changes in Alzheimer's Disease, Identified by Means of Linked Independent Component Analysis

Zsigmond Tamas Kincses[a,b], Daniel Hořínek[b], Nikoletta Szabó[a,b], Eszter Tóth[a], Gergő Csete[a], Irena Štěpán-Buksakowska[a,e], Jakub Hort[b,e] and László Vécsei[a,c,*]
[a]*Albert Szent-Györgyi Clinical Center, Department of Neurology, University of Szeged, Szeged, Hungary*
[b]*International Clinical Research Center, St. Anne's University Hospital Brno, Brno, Czech Republic*
[c]*Neuroscience Research Group of the Hungarian Academy of Sciences and University of Szeged, Szeged, Hungary*
[d]*Memory Disorders Clinic, Department of Neurology, Charles University in Prague, 2nd Faculty of Medicine and University Hospital Motol, Prague, Czech Republic*
[e]*Department of Radiology, Charles University, 2nd Medical Faculty and University Hospital Motol, Prague, Czech Republic*

Accepted 7 March 2013

Abstract. Several recent studies have indicated that white matter is affected in Alzheimer's disease (AD). Diffusion tensor imaging is a tool by which the white matter microstructure can be examined *in vivo*, and might offer a possibility for the identification of the pattern of white matter disintegration in AD. In the current analysis, we made use of a novel model-free analysis approach of linked independent component analysis to identify a motif of diffusion parameter alterations exemplifying AD. Analysis of the diffusion data of 16 AD patients and 17 age-matched healthy subjects revealed six independent components, two of which demonstrated differences between the patients and controls. Component #0 was dominated by axial diffusivity, but significant alterations in fractional anisotropy and mean and radial diffusivity were also detected. Alterations were found in regions of crossing of major white matter pathways, such as forceps, corona radiate, and superior longitudinal fascicle, as well as medio-temporal white matter. These results lend support to the coexistence of white matter disintegration of the late myelinating associating fibers and wallerian degeneration-related disintegration, in accordance with the retrogenesis and wallerian degeneration hypothesis.

Keywords: Alzheimer's disease, diffusion tensor imaging, linked independent component analysis, magnetic resonance imaging

INTRODUCTION

Alzheimer's disease (AD) is the most common type of dementia in the elderly. A recent report forecasted that the prevalence of AD was set to rise to 35.6 million people globally by 2010 [1, 2], with the imposition of an enormous financial burden. The key feature of the disease is the progressive deficit in several cognitive domains [3–7], paralleled by regionally specific brain atrophy [8–11] and by white matter disintegration [12] that leads to a functional disconnection of the cortical regions [13].

Structural magnetic resonance imaging (MRI) studies were shown to have high sensitivity and specificity in the diagnosis of AD [14, 15], but advanced MRI approaches have recently provided further insight into the pathomechanisms of the disease. Among those, diffusion-weighted MRI permits a quantification of water diffusion in the brain in a manner that reflects the tissue microstructure. Hence, it is an emerging approach for the identification of biomarkers of various disorders that affect the central nervous system

*Correspondence to: László Vécsei, MD, PhD, Department of Neurology, Albert Szent-Györgyi Clinical Center, University of Szeged, Semmelweis u. 6, 6725-Szeged, Hungary. E-mail: vecsei.laszlo@med.u-szeged.hu.

[16–19]. Various parameters of diffusion that are related to different aspects of the tissue microstructure, such as fractional anisotropy (FA), mean diffusivity (MD), and diffusivity parallel ($\lambda 1$) and perpendicular ($(\lambda 2 + \lambda 3)/2$) to the principal diffusion direction, are used to quantify diffusion.

A number of studies have revealed altered diffusion parameters in AD, and over the years, different approaches have been used to evaluate these parameters. Earlier investigations restricted the analysis to certain brain regions [20, 21], an approach that is highly hypothesis-driven, and cross-study comparisons are difficult. Later the analysis was extended to the whole brain using voxel-based morphometric style analysis [15, 22, 23]. However, the optimal analysis was compromised by the possible misalignment of FA images [24]. To overcome this registration issue, it was recommended that analyses should be restricted to the core of the fiber bundles, represented by the local FA maxima [12, 24].

Despite the undisputed merits of these studies, it has been argued that a combination of diffusion parameters should be evaluated together in order to identify disease-specific markers [18]. The patterns of various diffusion parameters have to be judged, together with the spatial pattern of the combination of these parameters. Standard approaches based on the general linear model framework are not well suited for this because the information relating to the different diffusion parameters is combined only at the point of interpretation. Model-free, exploratory data analysis methods offer a solution, by fusing data before statistical analysis in order to characterize multimodal variances across space [25]. Linked independent component analysis (ICA) was recently proposed to obtain independent components of multimodal variability [26]. Linked ICA automatically balances the information content of different modalities, finding subject loadings that produce statistically independent and non-Gaussian spatial maps across the modalities.

In the current study, we set out to identify the spatial pattern of the diffusion parameter motif characteristic of AD. We used linked ICA to decompose the data containing various diffusion parameters in the white matter skeleton representing the core of the fiber bundles.

METHODS

Subjects

A total of 16 subjects diagnosed with AD (median age $\pm$ SD: 77.5 ± 6.71 y) and 17 healthy controls (median age $\pm$ SD: 74 ± 8.4 y) were enrolled in the study. Age and gender was not significantly different in the two groups (age: Mann-Whitney test: $U = 84.5$, $z = -1.84$, $p = 0.063$; gender: $\chi^2(2, n = 33) = 3.51$, $p = 0.72$). All the AD patients were recruited by a neurologist from the Memory Disorders Unit, Department of Neurology (University Hospital Motol, Prague, Czech Republic). Clinical diagnosis was made in accordance with the EFNS guidelines [27]. Participants were evaluated by a neurologist who obtained medical history from the patient and caregiver, and performed the Mini-Mental State Examination (MMSE), Hachinski Ischemic Scale, and a neurological examination. Research assistants and study coordinators gathered other data including Geriatric Depression Scale, Activities of Daily Living, and additional personal and family history.

Table 1
Sociodemographic data of the subjects

	AD	Control
n	16	17
Age, median (SD)	77.5 (6.71)	74 (8.4)
Gender, male	5	7
MMSE, median (range)	21 (14–25)	30 (30)
Donepezil	9	n.a.
Rivastigmine	4	n.a.
Memantine	1	n.a.

MMSE, Mini-Mental State exam; n.a., not applicable.

All participants were administered a comprehensive neuropsychological evaluation. The psychometric battery covered the following cognitive areas: 1) verbal memory measured with the Auditory Verbal Learning Test trials 1–6 and Delayed Recall trial, Free and Cued Selective Reminding Test; 2) non-verbal memory measured with the Rey-Osterrieth Complex Figure Test-the Immediate Recall condition; 3) visuospatial function measured with the Rey-Osterrieth Complex Figure Test-the Copy condition; 4) executive function measured with the Trail Making Test B and Controlled Oral Word Association Test; 5) attention and working memory measured with the Backward Digit Span and Trail Making Test A; and 6) language measured with the Boston Naming Test.

Most of the subjects were either on a cholinesterase blocker or NMDA receptor blocker medication (4 rivastigmine, 9 donepezil, 1 memantine; see Table 1). Control subjects with normal cognition were recruited from among the family members of the patients and from the group who responded to an advertisement. All participating subjects underwent neurological and neuropsychological evaluation. The mean MMSE score was 20.18 (range: 14–25) for patients and 29.29

(range: 24–30) for controls. Concomitant diseases, such as hypertension, diabetes, and hypercholesterolemia were evenly represented in the two study groups. The exclusion criteria for patients and controls included illicit drug use and any major neurological or psychiatric disorder other than AD. All the subjects involved (or their guardians in the cases of demented patients) provided their written informed consent; approval for the study protocol was given by the local medical-ethical committee.

Data acquisition

MR imaging was carried out on a 3T GE MR scanner. 3D spoiled gradient echo images (FSPGR: TE: 4.1 ms, TR: 10.276 ms, matrix: 256 × 256, FOV: 25 × 25 cm, Flip angle: 15°, in-plane resolution: 1 × 1 mm, slice thickness: 1 mm) and 30 direction diffusion weighted images with 5 non-diffusion-weighted reference volumes (TE: 93.8 ms, TR: 16000 ms, matrix: 96 × 96, FOV: 23 × 23 cm, Flip angle: 90°, in-plane resolution: 2.4 × 2.4 mm slice thickness: 2.4 mm, b: 1000 s/m2, NEX: 2, ASSET) were acquired for all subjects.

Image analysis

Diffusion data were corrected for eddy currents and movement artifacts by 12 degrees of freedom affine linear registration to the first non-diffusion-weighted reference image [28]. Diffusion tensors at each voxel were fitted by the algorithm included in the FMRIB's Diffusion Toolbox (FDT) of the FMRIB's Software Library (FSL v. 4.0, http://www.fmrib.ox.ac.uk/fsl; [29]). FA, MD, and diffusivity parallel ($\lambda 1$) and perpendicular (($\lambda 2 + \lambda 3$)/2) to the principal diffusion direction were computed for the whole brain. In order to reduce the possible errors arising from misalignment of the images, we used the Tract Based Spatial Statistics (TBSS) method [24]. For all subjects, the FA data were aligned into a common space chosen to be the best target from all FA images, using the non-linear registration tool FNIRT [30], which uses a b-spline representation of the registration warp field [31]. A mean FA skeleton was derived from the mean FA image, which represents the centers of all tracts common to the group. The aligned FA data for each subject was then projected onto this skeleton and thresholded at 0.2 FA. Similarly to FA, the MD, axial, and radial diffusivity images were also warped to the thresholded mean FA skeleton image. For computational reasons, images were downsampled to an isotropic resolution of 2 mm. The resulting images were fed into the linked ICA.

Linked independent component analysis

Linked ICA is an exploratory data analysis approach for the fusion of information from several different imaging modalities. The approach was described in detail earlier [26]. The main aim of the analysis is to identify combined group level features of the multimodal data that reflect a biophysically plausible form of variability. The resulting components consist of *subject loading*, which indicates how much the given combination of *modalities* across *space* is expressed in individual subjects. The original, full version of the analysis decomposes the multimodal data from different modality groups with identical spatial organization in a modality group over modalities. In the current analysis, we used a restricted version of the approach, with only a single modality group of different diffusion parameters in the FA skeleton. The decomposition results in a trilinear factorization of the data:

$$y_{n,t,r} = \sum_{i=1}^{L} X_{n,i} W_{t,i} H_{i,r} + E_{n,t,r} \qquad (1)$$

where in an n voxel space, $X_{n,i}$ is the spatial map for component i, $W_{t,i}$ is the modality weighting for component i in modality t, and $H_{i,r}$ is the weight for component i in subject r. Uncorrelated Gaussian residuals are assumed, with the modality-dependent noise precision λ_t:

$$E_{n,t,r} \sim N(0, 1/\lambda_t). \qquad (2)$$

To adapt to different scalings of the signal in each modality, an automatic relevance determination [32] prior is used on the modality courses (W).

The matrices are optimized to find estimates of the generative model of Eq. 1 such that the spatial maps are maximally non-Gaussian. The spatial patterns were converted to pseudo-Z-statistics by accounting for the scaling of the variables and the SNR in that modality. Images were thresholded at the pseudo-z-value of 3.1 or 2.3.

RESULTS

We decomposed the combined data of 16 patients and 17 controls with linked ICA into six independent components. Out of the six components, only two showed different subject loadings in the two investigated groups (IC 0: $p < 0.044$, IC 3: $p < 0.0027$).

Table 2
Significant clusters in component #0. Side of the cluster (L-left, R-right), standard space coordinates in mm, z values for fractional anisotropy (FA), mean diffusivity (MD), axial (L1) and perpendicular (L23) diffusivity is given in the consecutive columns. The indicated peak statistical significances are based on axial diffusivity

Axial diffusivity	Side	X	Y	Z	FA	MD	L1	L23
Forceps minor, anterior corona radiate	L	−22	8	32	–	3.86	**5.71**	–
Forceps minor, anterior corona radiata	R	16	14	30	–	5.35	**6.98**	4.48
Forceps major, posterior corona radiata	L	−24	−40	26	−3.9	18.8	**13.7**	16.4
Forceps major, posterior corona radiata	R	24	−38	32	–	7.47	**9.85**	3.1
Corona radiata	L	−26	−24	34	–	–	**8.09**	–
Inferior fronto-occipital fasciculus versus posterior thalamic radiation	L	−30	−32	12	–	–	**4.95**	–
Superior longitudinal fasciculus corona radiata	R	34	−42	28	–	4.35	**5.39**	–
Uncinate fasciculus	L	−36	−4	−24	–	–	**4.21**	–
Corona radiata	R	28	−14	16	–	–	**4.91**	–
External capsule	R	36	−12	24	–	–	**4.87**	–
Superior longitudinal fasciculus	L	−26	−38	26	−3.1	17.3	**13.7**	14.4
Inferior longitudinal fasciculus	R	38	−24	−4	–	3.35	**3.66**	–
Anterior limb internal capsule	R	16	12	0	–	4.85	**4.83**	–
Anterior limb internal capsule	L	−18	8	6	–	–	**3.63**	–
Paraamygdalar white matter	L	−28	−12	−8	–	3.92	**4.61**	–
Paraamygdalar white matter	R	28	−10	−10	–	3.8	**4.64**	–
Cingulum	L	−28	−40	−8	–	14.1	**9.95**	12.5
Fornix	L	−2	8	−2	–	3.46	**5.29**	–

The subject loadings were not correlated with the cognitive function of the patients as measured by the MMSE.

IC 0 was dominated by axial diffusivity (39%), but to a smaller degree, MD (27%), FA (14%), and perpendicular diffusivity (20%) also made significant contribution.

In the spatial map, increased axial diffusivity was found in patients in several regions where fibers are crossing: forceps major and minor and corona radiata, superior longitudinal fascicle and corona radiata (in Table 2 both of these structures are indicated). Smaller clusters were found with similar diffusion alterations in the parahippocampal (putative cingulum bundle) and paraamygdalar white matter, fornix, uncinate fasciculus, and in the thalami. Importantly fibers of the internal capsule were spared.

Increased axial diffusivity was accompanied by increased MD in most of the regions described above. Additionally some smaller clusters of increased MD were detected in juxtacortical white matter. Similarly, increased perpendicular diffusivity was found in patients in similar regions identified with the axial diffusivity alterations. The peak of statistical significance in case of perpendicular diffusivity was in the close vicinity that of axial diffusivity, but in most of the cases not right on the same spot.

Decreased FA was detected in two larger clusters in the forceps major bilaterally (right: $x = -28$ mm, $y = -60$ mm, $z = 12$ mm, $Z_{FA} = -6.1$, $Z_{MD} = 3.79$, $Z_{RD} = 6.73$; left$x = 26$ mm, $y = -52$ mm, $z = 10$ mm, $Z_{FA} = -4.26$, $Z_{MD} = 4.11$, $Z_{RD} = 5.66$). Some smaller clusters were detected in the juxtacortical white matter.

IC 3 was also dominated by axial diffusivity (52%) and MD (29%). FA and perpendicular diffusivity had only minor contribution (3% and 15% respectively).

The spatial map of increased axial diffusivity indicated a small cluster in the left parahippocampal white matter (putative cingulum bundle; $x = -26$ mm, $y = -32$ mm, $z = -16$ mm, $Z_{MD} = 2.75$, $Z_{AD} = 2.39$). A few single voxel size differences were found in various bilateral, frontal, and temporal regions.

The spatial map of the MD (increased in patients) depicted a left precuneal juxtacortical white matter cluster ($x = -18$ mm, $y = -62$ mm, $z = 30$ mm, $Z_{MD} = 2.83$), a left cluster in the left cingulum bundle—the same spot as indicated by the axial diffusivity. Small clusters of increased MD were found in the anterior temporal white matter (possibly inferior longitudinal fascicle) bilaterally (left: $x = -40$ mm, $y = -10$ mm, $z = -30$ mm, $Z_{MD} = 2.4$; right: $x = 40$ mm, $y = -10$ mm, $z = -28$ mm, $Z_{MD} = 2.54$). A few single voxel differences were detected in the frontal, parietal, temporal, occipital white matter, bilateral anterior commissure, and in the left thalamus.

The component did not indicate differences in FA or perpendicular diffusivity.

DISCUSSION

In the current study we used multivariate analysis to identify the motif of diffusion parameter changes

in AD. One of the most crucial finding of this analysis was that diffusion alterations in AD are dominated by increased axial diffusivity. The increased axial diffusivity, which was paralleled by increased mean and perpendicular diffusivity, was found in the intersection of major white matter fiber bundles such as forceps major and minor, corona radiate, and superior longitudinal fascicle. Importantly the alterations spared the internal capsulae. Similar changes were found in the medio-temporal structures.

There are two models of white matter disintegration in AD. The retrogenesis model posits that white matter disintegration is the reverse of the myelogenesis [33]. The small-diameter fibers that are myelinated last in the neocortical association and the allocortical fibers are the first to be affected during the progression of the disease [34]. An alternative hypothesis considers that the white matter disintegration is related to the wallerian degeneration due to cortical neuronal degeneration [35]. Our results, which revealed white matter disintegration in the association fibers as well as in parahippocampal white matter, indicate that the two hypotheses might exist in parallel.

Similar data on AD patients were earlier analyzed by Groves and colleagues [26] with linked ICA in the seminal paper describing the method. However, that analysis was different in additionally considering the gray matter atrophy besides the microstructural alterations measured with diffusion MRI. Hence, in their analysis, the components described complex variations of the gray and white matter, which were expressed in the same way in individual subjects. With that, they hypothesized that white matter disintegration is related to cortical atrophy or at least co-occurs with similar dynamics in patients (wallerian degeneration model). While this is reasonable, it might also be necessary to consider gray matter atrophy-independent microstructural changes (retrogenesis model). In their analysis component #2 of the flat, concatenated and linked ICA identified widespread cortical atrophy and co-occurring white matter disintegration. In contrast, component #11 of the Groves analysis identified FA and MD alterations mainly in the callosal fibers without cortical atrophy. In our analysis, neocortical association fibers and the medial temporal white matter were also affected, which may point to the validity of both models. However, it should be emphasized that late myelinating fibers connect to the medio-temporal structures [36].

While it is generally accepted that the primary pathology is in the gray matter, it has also become clear that the cognitive dysfunction in AD is also related to disconnection [37]. This has been confirmed in several *in vivo* human diffusion [12] and functional MRI studies [13, 38], and in human [39] and animal [40] histological investigations. Moreover, it is known that amyloid-β protein aggregates can also be found in the white matter [41] and regionally specific myelination abnormalities can be detected prior to the development of tau and amyloid pathology in an animal model of AD. It was reported recently that the amyloid-β_{1-42} oligomer inhibits myelin formation *in vivo* [42]. Oligodendrocytes have been demonstrated to be susceptible to amyloid-β [43] and oxidative stress [44], factors that are crucial in the pathogenesis of AD [45].

Thus, diffusion MRI-detected parameter alterations have frequently been described in AD. While the reported spatial distribution of such alterations is variable, most is probably the consequence of methodological differences; callosal and medio-temporal disintegration are often reported features [22, 46–50]. Furthermore, correlation of cognitive performance with diffusion parameters was recently investigated with univariate approaches [51–53]. In a recent TBSS study investigating several cognitive measures, only memory composite was correlated with FA when AD and mild cognitive impairment patients were analyzed together but not for AD patients separately [51]. Similarly, in our study no correlation was found between the expression of the components in individual subjects (subject loadings) and the MMSE scores. It is important to point out MMSE is a general measure of cognitive performance and does not test a single specific cognitive function which could be correlated with a focal structural alteration.

Previous studies have indicated that the different patterns of the diffusion parameter alterations may be associated with different pathological changes in the white matter. The alterations of axial and radial diffusivity in mouse models of multiple sclerosis have been suggested to relate to axon or myelin damage, respectively [54–56]. One mouse model study revealed a decreased FA in transected nerves, the FA returning toward the normal in the course of axonal regeneration. Additionally, the FA and axial diffusivity correlated significantly with the total axon count [57]. In the optic nerve of mice, a significantly decreased axial diffusivity was observed 3 days after retinal ischemia without any detectable changes in radial diffusivity, which was consistent with histological finding of significant axonal degeneration without demyelination. Consistent with the histological finding of myelin degeneration, an increase in radial diffusivity was observed 5 days after ischemia [58]. The myelin content in the postmortem human brain, prior to and

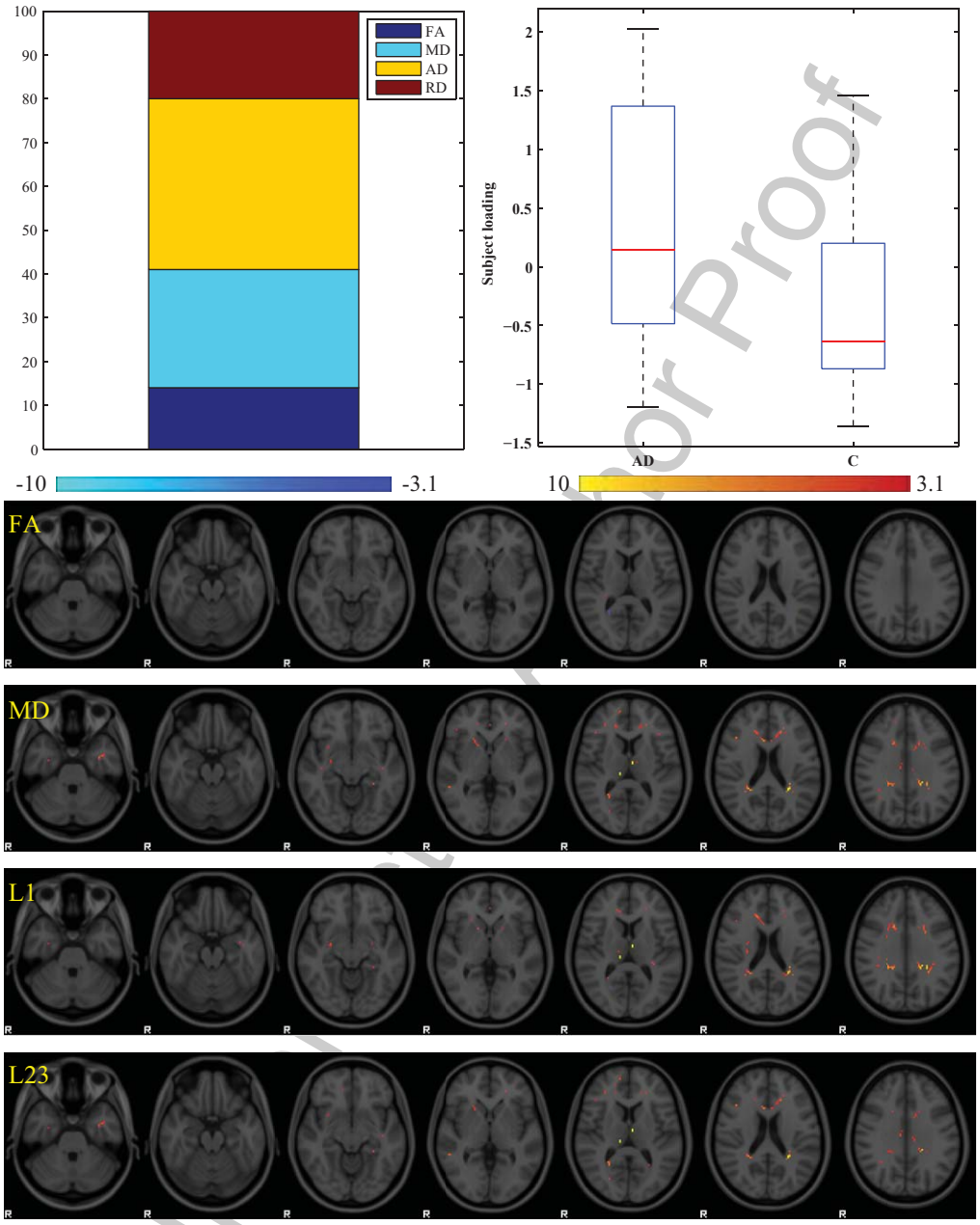

Fig. 1. Summary graph of component #0. Subject loadings were different between AD patients and healthy controls ($p < 0.044$, higher in patients, top-right boxplot). The component was mainly driven by the axial diffusivity (top-left barplot). Statistical images are overlaid on MNI152 standard brain. Blue-to-light blue color signifies a reduction, red-to-yellow an increment of the given parameter (FA, fractional anisotropy; MD, mean diffusivity; L1, axial diffusivity; L23, perpendicular diffusivity). Images are thresholded at z = 3.1. Color bars reflect pseudo-z values.

after fixation, was predicted by the changes in radial diffusivity, together with FA and MD [59]. A further possibility behind the increased axial diffusivity might be the selective degeneration of the weaker of the crossing fibers [60]. In the current study, the identified components were most strongly influenced by the axial diffusivity. This might suggest that axonal loss is the key pathological process. On the other hand, other diffusion parameter changes were also significantly included in the independent components. At this stage, the pathological relevance of these findings cannot be unanimously concluded.

While it is crucially important to understand the pathological relevance of the diffusion alterations

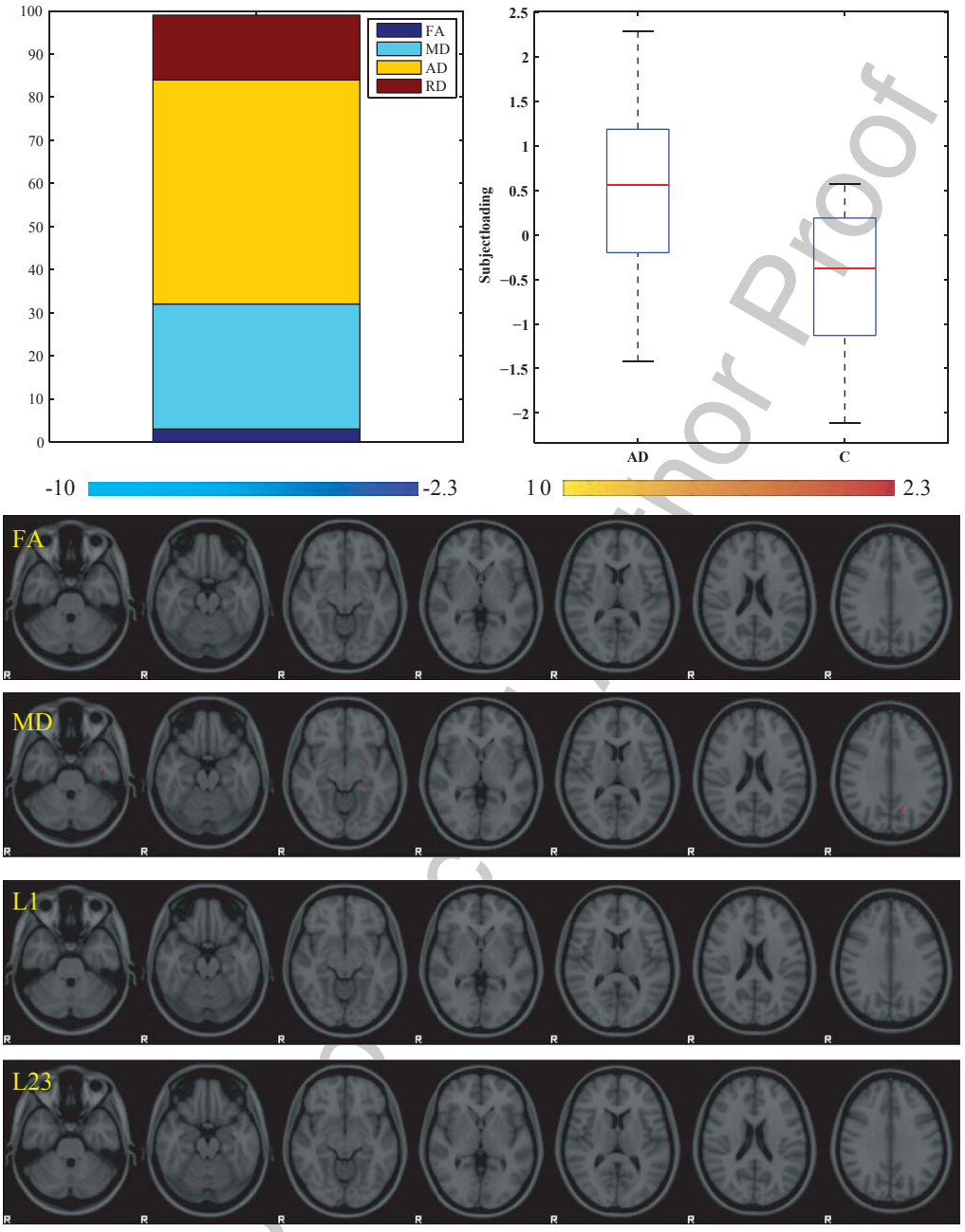

Fig. 2. Summary graph of component #3. Subject loadings were different between AD patients and healthy controls ($p < 0.0027$, higher in patients, top-right boxplot). The component was mainly driven by the axial diffusivity (top-left barplot). Statistical images are overlaid on MNI152 standard brain. Blue-to-light blue color signifies a reduction, red-to-yellow an increment of the given parameter (FA, fractional anisotropy; MD, mean diffusivity; L1, axial diffusivity; L23, perpendicular diffusivity). Images are thresholded at z = 2.3. Color bars reflect pseudo-z values.

in AD, if further studies could confirm the results and extend these findings in longitudinal investigations, diffusion MRI could be a potential biomarker in studies testing putative neuroprotective treatments.

ACKNOWLEDGMENTS

This research was supported by grant IGA NS 10331 by the International Research Center (FNUSA-ICRC, no. CZ.1.05/1.1.00/02.0123) from the European

Regional Development Fund, the "Neuroscience Research Group of the Hungarian Academy of Sciences and University of Szeged" the OTKA PD104715, TÁMOP-4.2.2.A-11/1/KONV-2012-0073 and TÁMOP-4.2.2/B-10/1-2010-0012 grant. Dr. Kincses was supported by the Bolyai Scholarship Programme of the Hungarian Academy of Sciences. We thank David Durham for help with English editing.

Authors' disclosures available online (http://www.j-alz.com/disclosures/view.php?id=1706)

REFERENCES

[1] Dartigues JF (2009) Alzheimer's disease: A global challenge for the 21st century. *Lancet Neurol* **8**, 1082-1083.

[2] Prince M, Jackson J (2009) World Alzheimer Report. *Alzheimer Disease International*, http://www.alz.co.uk/research/files/WorldAlzheimerReport.pdf.

[3] Keri S, Kalman J, Kelemen O, Benedek G, Janka Z (2001) Are Alzheimer's disease patients able to learn visual prototypes? *Neuropsychologia* **39**, 1218-1223.

[4] Antal A, Keri S, Kincses T, Kalman J, Dibo G, Benedek G, Janka Z, Vecsei L (2002) Corticostriatal circuitry mediates fast-track visual categorization. *Brain Res Cogn Brain Res* **13**, 53-59.

[5] Hoffmann I, Nemeth D, Dye CD, Pakasi M, Irinyi T, Kalman J (2010) Temporal parameters of spontaneous speech in Alzheimer's disease. *Int J Speech Lang Pathol* **12**, 29-34.

[6] Waltz JA, Knowlton BJ, Holyoak KJ, Boone KB, Back-Madruga C, McPherson S, Masterman D, Chow T, Cummings JL, Miller BL (2004) Relational integration and executive function in Alzheimer's disease. *Neuropsychology* **18**, 296-305.

[7] Salmon DP, Butters N, Chan AS (1999) The deterioration of semantic memory in Alzheimer's disease. *Can J Exp Psychol* **53**, 108-117.

[8] Filippini N, Rao A, Wetten S, Gibson RA, Borrie M, Guzman D, Kertesz A, Loy-English I, Williams J, Nichols T, Whitcher B, Matthews PM (2009) Anatomically-distinct genetic associations of APOE epsilon4 allele load with regional cortical atrophy in Alzheimer's disease. *Neuroimage* **44**, 724-728.

[9] Zarei M, Patenaude B, Damoiseaux J, Morgese C, Smith S, Matthews PM, Barkhof F, Rombouts S, Sanz-Arigita E, Jenkinson M (2010) Combining shape and connectivity analysis: An MRI study of thalamic degeneration in Alzheimer's disease. *Neuroimage* **49**, 1-8.

[10] Zarei M, Damoiseaux JS, Morgese C, Beckmann CF, Smith SM, Matthews PM, Scheltens P, Rombouts SA, Barkhof F (2009) Regional white matter integrity differentiates between vascular dementia and Alzheimer disease. *Stroke* **40**, 773-779.

[11] Smith SM, Rao A, De Stefano N, Jenkinson M, Schott JM, Matthews PM, Fox NC (2007) Longitudinal and cross-sectional analysis of atrophy in Alzheimer's disease: Cross-validation of BSI, SIENA and SIENAX. *Neuroimage* **36**, 1200-1206.

[12] Liu Y, Spulber G, Lehtimaki KK, Kononen M, Hallikainen I, Grohn H, Kivipelto M, Hallikainen M, Vanninen R, Soininen H (2011) Diffusion tensor imaging and tract-based spatial statistics in Alzheimer's disease and mild cognitive impairment. *Neurobiol Aging* **32**, 1558-1571.

[13] Delbeuck X, Van der Linden M, Collette F (2003) Alzheimer's disease as a disconnection syndrome? *Neuropsychol Rev* **13**, 79-92.

[14] Bloudek LM, Spackman DE, Blankenburg M, Sullivan SD (2011) Review and meta-analysis of biomarkers and diagnostic imaging in Alzheimer's disease. *J Alzheimers Dis* **26**, 627-645.

[15] Teipel SJ, Wegrzyn M, Meindl T, Frisoni G, Bokde AL, Fellgiebel A, Filippi M, Hampel H, Kloppel S, Hauenstein K, Ewers M (2012) Anatomical MRI and DTI in the diagnosis of Alzheimer's disease: A European multicenter study. *J Alzheimers Dis* **31**(Suppl 3), S33-S47.

[16] Szabo N, Kincses ZT, Pardutz A, Tajti J, Szok D, Tuka B, Kiraly A, Babos M, Voros E, Bomboi G, Orzi F, Vecsei L (2012) White matter microstructural alterations in migraine: A diffusion-weighted MRI study. *Pain* **153**, 651-656.

[17] Rosas HD, Tuch DS, Hevelone ND, Zaleta AK, Vangel M, Hersch SM, Salat DH (2006) Diffusion tensor imaging in presymptomatic and early Huntington's disease: Selective white matter pathology and its relationship to clinical measures. *Mov Disord* **21**, 1317-1325.

[18] O'Dwyer L, Lamberton F, Bokde AL, Ewers M, Faluyi YO, Tanner C, Mazoyer B, O'Neill D, Bartley M, Collins DR, Coughlan T, Prvulovic D, Hampel H (2011) Multiple indices of diffusion identifies white matter damage in mild cognitive impairment and Alzheimer's disease. *PLoS One* **6**, e21745.

[19] Hattori T, Ito K, Aoki S, Yuasa T, Sato R, Ishikawa M, Sawaura H, Hori M, Mizusawa H (2012) White matter alteration in idiopathic normal pressure hydrocephalus: Tract-based spatial statistics study. *AJNR Am J Neuroradiol* **33**, 97-103.

[20] Bozzali M, Falini A, Franceschi M, Cercignani M, Zuffi M, Scotti G, Comi G, Filippi M (2002) White matter damage in Alzheimer's disease assessed *in vivo* using diffusion tensor magnetic resonance imaging. *J Neurol Neurosurg Psychiatry* **72**, 742-746.

[21] Choi SJ, Lim KO, Monteiro I, Reisberg B (2005) Diffusion tensor imaging of frontal white matter microstructure in early Alzheimer's disease: A preliminary study. *J Geriatr Psychiatry Neurol* **18**, 12-19.

[22] Xie S, Xiao JX, Gong GL, Zang YF, Wang YH, Wu HK, Jiang XX (2006) Voxel-based detection of white matter abnormalities in mild Alzheimer disease. *Neurology* **66**, 1845-1849.

[23] Medina D, DeToledo-Morrell L, Urresta F, Gabrieli JD, Moseley M, Fleischman D, Bennett DA, Leurgans S, Turner DA, Stebbins GT (2006) White matter changes in mild cognitive impairment and AD: A diffusion tensor imaging study. *Neurobiol Aging* **27**, 663-672.

[24] Smith SM, Jenkinson M, Johansen-Berg H, Rueckert D, Nichols TE, Mackay CE, Watkins KE, Ciccarelli O, Cader MZ, Matthews PM, Behrens TE (2006) Tract-based spatial statistics: voxelwise analysis of multi-subject diffusion data. *Neuroimage* **31**, 1487-1505.

[25] Teipel SJ, Stahl R, Dietrich O, Schoenberg SO, Perneczky R, Bokde AL, Reiser MF, Moller HJ, Hampel H (2007) Multivariate network analysis of fiber tract integrity in Alzheimer's disease. *Neuroimage* **34**, 985-995.

[26] Groves AR, Beckmann CF, Smith SM, Woolrich MW (2011) Linked independent component analysis for multimodal data fusion. *Neuroimage* **54**, 2198-2217.

[27] Hort J, O'Brien JT, Gainotti G, Pirttila T, Popescu BO, Rektorova I, Sorbi S, Scheltens P (2010) EFNS guidelines for the diagnosis and management of Alzheimer's disease. *Eur J Neurol* **17**, 1236-1248.

[28] Jenkinson M, Smith S (2001) A global optimisation method for robust affine registration of brain images. *Med Image Anal* **5**, 143-156.

[29] Smith SM, Jenkinson M, Woolrich MW, Beckmann CF, Behrens TE, Johansen-Berg H, Bannister PR, De Luca M, Drobnjak I, Flitney DE, Niazy RK, Saunders J, Vickers J, Zhang Y, De Stefano N, Brady JM, Matthews PM (2004) Advances in functional and structural MR image analysis and implementation as FSL. *Neuroimage* **23**(Suppl 1), S208-S219.

[30] Andersson JLR, Jenkinson M, Smith S (2007) Non-linear optimization. *FMRIB Technical Report*, Oxford.

[31] Rueckert D, Sonoda LI, Hayes C, Hill DL, Leach MO, Hawkes DJ (1999) Nonrigid registration using free-form deformations: Application to breast MR images. *IEEE Trans Med Imaging* **18**, 712-721.

[32] Wipf D, Nagarajan S (2008) A new view of automatic relevance determination. In *Advances in Neural Information Processing Systems 20*, Platt JC, Koller D, Singer Y, Roweis S, eds. MIT Press, Cambridge.

[33] Reisberg B, Franssen EH, Hasan SM, Monteiro I, Boksay I, Souren LE, Kenowsky S, Auer SR, Elahi S, Kluger A (1999) Retrogenesis: Clinical, physiologic, and pathologic mechanisms in brain aging, Alzheimer's and other dementing processes. *Eur Arch Psychiatry Clin Neurosci* **249**(Suppl 3), 28-36.

[34] Bartzokis G. (2004) Age-related myelin breakdown: A developmental model of cognitive decline and Alzheimer's disease. *Neurobiol Aging* **25**, 5-18; author reply 49-62.

[35] Coleman M (2005) Axon degeneration mechanisms: Commonality amid diversity. *Nat Rev Neurosci* **6**, 889-898.

[36] Brun A, Englund E (1986) A white matter disorder in dementia of the Alzheimer type: A pathoanatomical study. *Ann Neurol* **19**, 253-262.

[37] Gunning-Dixon FM, Raz N (2000) The cognitive correlates of white matter abnormalities in normal aging: A quantitative review. *Neuropsychology* **14**, 224-232.

[38] Greicius MD, Srivastava G, Reiss AL, Menon V (2004) Default-mode network activity distinguishes Alzheimer's disease from healthy aging: Evidence from functional MRI. *Proc Natl Acad Sci U S A* **101**, 4637-4642.

[39] Stokin GB, Lillo C, Falzone TL, Brusch RG, Rockenstein E, Mount SL, Raman R, Davies P, Masliah E, Williams DS, Goldstein LS (2005) Axonopathy and transport deficits early in the pathogenesis of Alzheimer's disease. *Science* **307**, 1282-1288.

[40] Desai MK, Sudol KL, Janelsins MC, Mastrangelo MA, Frazer ME, Bowers WJ (2009) Triple-transgenic Alzheimer's disease mice exhibit region-specific abnormalities in brain myelination patterns prior to appearance of amyloid and tau pathology. *Glia* **57**, 54-65.

[41] Roher AE, Weiss N, Kokjohn TA, Kuo YM, Kalback W, Anthony J, Watson D, Luehrs DC, Sue L, Walker D, Emmerling M, Goux W, Beach T (2002) Increased A beta peptides and reduced cholesterol and myelin proteins characterize white matter degeneration in Alzheimer's disease. *Biochemistry* **41**, 11080-11090.

[42] Horiuchi M, Maezawa I, Itoh A, Wakayama K, Jin LW, Itoh T, Decarli C (2012) Amyloid beta1-42 oligomer inhibits myelin sheet formation *in vitro*. *Neurobiol Aging* **33**, 499-509.

[43] Zeng C, Lee JT, Chen H, Chen S, Hsu CY, Xu J (2005) Amyloid-beta peptide enhances tumor necrosis factor-alpha-induced iNOS through neutral sphingomyelinase/ceramide pathway in oligodendrocytes. *J Neurochem* **94**, 703-712.

[44] Deng W, Wang H, Rosenberg PA, Volpe JJ, Jensen FE (2004) Role of metabotropic glutamate receptors in oligodendrocyte excitotoxicity and oxidative stress. *Proc Natl Acad Sci U S A* **101**, 7751-7756.

[45] Kincses ZT, Toldi J, Vecsei L (2010) Kynurenines, neurodegeneration and Alzheimer's disease. *J Cell Mol Med* **14**, 2045-2054.

[46] Stricker NH, Schweinsburg BC, Delano-Wood L, Wierenga CE, Bangen KJ, Haaland KY, Frank LR, Salmon DP, Bondi MW (2009) Decreased white matter integrity in late-myelinating fiber pathways in Alzheimer's disease supports retrogenesis. *Neuroimage* **45**, 10-16.

[47] Damoiseaux JS, Smith SM, Witter MP, Sanz-Arigita EJ, Barkhof F, Scheltens P, Stam CJ, Zarei M, Rombouts SA (2009) White matter tract integrity in aging and Alzheimer's disease. *Hum Brain Mapp* **30**, 1051-1059.

[48] Salat DH, Tuch DS, van der Kouwe AJ, Greve DN, Pappu V, Lee SY, Hevelone ND, Zaleta AK, Growdon JH, Corkin S, Fischl B, Rosas HD (2010) White matter pathology isolates the hippocampal formation in Alzheimer's disease. *Neurobiol Aging* **31**, 244-256.

[49] Zhang Y, Schuff N, Jahng GH, Bayne W, Mori S, Schad L, Mueller S, Du AT, Kramer JH, Yaffe K, Chui H, Jagust WJ, Miller BL, Weiner MW (2007) Diffusion tensor imaging of cingulum fibers in mild cognitive impairment and Alzheimer disease. *Neurology* **68**, 13-19.

[50] Rose SE, McMahon KL, Janke AL, O'Dowd B, de Zubicaray G, Strudwick MW, Chalk JB (2006) Diffusion indices on magnetic resonance imaging and neuropsychological performance in amnestic mild cognitive impairment. *J Neurol Neurosurg Psychiatry* **77**, 1122-1128.

[51] Bosch B, Arenaza-Urquijo EM, Rami L, Sala-Llonch R, Junque C, Sole-Padulles C, Pena-Gomez C, Bargallo N, Molinuevo JL, Bartres-Faz D (2012) Multiple DTI index analysis in normal aging, amnestic MCI and AD. Relationship with neuropsychological performance. *Neurobiol Aging* **33**, 61-74.

[52] Fellgiebel A, Schermuly I, Gerhard A, Keller I, Albrecht J, Weibrich C, Muller MJ, Stoeter P (2008) Functional relevant loss of long association fibre tracts integrity in early Alzheimer's disease. *Neuropsychologia* **46**, 1698-1706.

[53] Huang J, Auchus AP (2007) Diffusion tensor imaging of normal appearing white matter and its correlation with cognitive functioning in mild cognitive impairment and Alzheimer's disease. *Ann N Y Acad Sci* **1097**, 259-264.

[54] Budde MD, Kim JH, Liang HF, Russell JH, Cross AH, Song SK (2008) Axonal injury detected by *in vivo* diffusion tensor imaging correlates with neurological disability in a mouse model of multiple sclerosis. *NMR Biomed* **21**, 589-597.

[55] Song SK, Yoshino J, Le TQ, Lin SJ, Sun SW, Cross AH, Armstrong RC (2005) Demyelination increases radial diffusivity in corpus callosum of mouse brain. *Neuroimage* **26**, 132-140.

[56] Sun SW, Liang HF, Schmidt RE, Cross AH, Song SK (2007) Selective vulnerability of cerebral white matter in a murine model of multiple sclerosis detected using diffusion tensor imaging. *Neurobiol Dis* **28**, 30-38.

[57] Lehmann HC, Zhang J, Mori S, Sheikh KA (2010) Diffusion tensor imaging to assess axonal regeneration in peripheral nerves. *Exp Neurol* **223**, 238-244.

[58] Song SK, Sun SW, Ju WK, Lin SJ, Cross AH, Neufeld AH (2003) Diffusion tensor imaging detects and differentiates axon and myelin degeneration in mouse optic nerve after retinal ischemia. *Neuroimage* **20**, 1714-1722.

[59] Schmierer K, Wheeler-Kingshott CA, Tozer DJ, Boulby PA, Parkes HG, Yousry TA, Scaravilli F, Barker GJ, Tofts PS,

Miller DH (2008) Quantitative magnetic resonance of post-mortem multiple sclerosis brain before and after fixation. *Magn Reson Med* **59**, 268-277.

[60] Douaud G, Jbabdi S, Behrens TE, Menke RA, Gass A, Monsch AU, Rao A, Whitcher B, Kindlmann G, Matthews PM, Smith S (2012) DTI measures in crossing-fibre areas: Increased diffusion anisotropy reveals early white matter alteration in MCI and mild Alzheimer's disease. *Neuroimage* **55**, 880-890.